

Advanced Sensors and Instrumentation

Issue 17 • July 2022

ASI Program Update

Daniel Nichols
Department of Energy



It has been 11 years since the Advanced Sensors and Instrumentation (ASI) program was first implemented in fiscal year (FY) 2011. The program has continued to foster collaborations across national laboratories, universities, and U.S. companies, generating notable accomplishments in the development of instrumentation and control (I&C) technologies, some of which are highlighted in this newsletter. Several ongoing geopolitical conflicts this year have revealed the fragility of the global energy market, emphasizing the need for more secure energy supply chains. Nuclear power shows promise for

providing energy security while promoting clean energy generation. The ASI program continues to develop the next generation of highly capable sensors and instrumentation in support of the continued operations of the existing nuclear reactor fleet, while also enabling the deployment of next-generation advanced nuclear reactors. The Advanced Sensor and Instrumentation program has demonstrated adaptability and innovation while continuing to support the missions of the Department of Energy (DOE) and the DOE Office of Nuclear Energy (DOE NE). The program will foster further stakeholder engagement by seeking out new opportunities for investment and collaboration, and by identifying research and development progress in other industries—progress leverageable for the advancement of nuclear energy.

1. ASI Program Update..... p. 1	6. Additive Manufactured Strain Gauges for Structural Health Monitoring p. 12
2. Radiation-resistant Digitizer for Inside Nuclear Reactor Containment. p. 2	7. Techno-Economic Assessment of a Multi-Band Heterogenous Wireless Network Architecture for Nuclear Power Plants..... p. 15
3. Development of Drift Models for High-Temperature Nuclear Thermocouples p. 4	8. Design and Prototyping of Advanced Control Systems for Advanced Reactors Operating in the Future Electric Grid p. 18
4. A Liquid Metal Laser Ultrasound Transmitter for High-Temperature NDT p. 7	9. Novel Cameras for Experiments Inside Nuclear Reactors p. 22
5. Printed High-Temperature Irradiation-Resistant Thermocouples for Real-time Monitoring of Nuclear Reactor Components..... p. 10	

For more program information, including recent publications, please visit www.asi.inl.gov



Radiation-resistant Digitizer for Use Inside Nuclear Reactor Containment

K.C. Goetz

Oak Ridge National Laboratory

Brian Jaques

Oak Ridge National Laboratory

Daniel C. Sweeney

Oak Ridge National Laboratory

N. Dianne Bull Ezell

Oak Ridge National Laboratory

Introduction

High-radiation and high-temperature environments represent notoriously detrimental conditions for electronics. Nevertheless, instrumentation and controls (I&Cs) are of critical importance for the safe operation of nuclear reactors, and for the validity of scientific experiments conducted within these reactors. Traditionally, sensors used in these types of extreme environments operate with a bare minimum of powered components, resulting in small signals (nA– μ A range) that are transmitted through long metal cabling. Long cables are prone to noise caused by electromagnetic interference (EMI) and loss of the desired signal as a result of the cable's inherent capacitance.

The remaining signal is small and noisy. The front-end digitizer (FrEnD) (see the block diagram in *Figure 1*) seeks to address these issues by placing a radiation-resistant analog front end (AFE) within the reactor containment, followed by immediate signal digitization and transmission, via optical fiber, outside the containment and over to an instrument room. Early signal preamplification and digitization help maintain signal integrity, while optical transmission renders the system immune to induced noise across the cable length. FrEnD can also read out an entire I&C suite for up to four different sensors over a single fiber optic cable. This includes thermocouples, self-powered neutron detectors (SPNDs), self-powered gamma detectors (SPGDs), thermistors, and fission chambers operating in current mode. The end result is an extremely flexible high-fidelity system that requires fewer penetrations into the reactor containment than is the case with traditional systems.



Radiation Resistance of FrEnD

FrEnD is radiation-resistant by design. The AFE and transmission circuitry were designed using as few components as possible in order to minimize potential failure sites, and junction-gate field effect transistors (JFETs) were chosen for their natural radiation resistance. Solid-state semiconductor transistors are the most common point of failure in electronic circuits exposed to high-radiation environments. Field-effect transistors are sensitive to the charges produced by ionizing radiation. Often these charges become trapped within the forbidden gap in insulators, leading to erroneous operation of the transistors (e.g., threshold voltage and transconductance variations). In large ionizing radiation fluxes, the sudden surge of produced and trapped charges leads to erroneous bit-flips in digital logic devices, referred to as single-event effects, single-event upsets, and single-event latchups. Ionizing radiation also induces stray currents in semiconductors and insulators which influence operation of transistors. Neutrons introduce displacement damage, which creates transmutation effects as well as vacancies in the semiconductor lattice structure, altering the device's dopant profile. Neutron activation also leads to the production of secondary ionization trails, which often lead to single-event burnout and single-event gate rupture. Both of these failure modes are fatal to the device. Of the existing commercially available solid-state semiconductors, JFETs are less sensitive to ionizing radiation, due to the absence of the insulating gate and the limited interfering surface effects typically created by insulating overlays. As such, the AFE of FrEnD was designed using low-cost discrete JFETs for the proof-of-principle prototype design. However, the chosen silicon-based JFETs have not yet been verified against neutron irradiation and are not expected to exceed the state-of-the-art neutron fluence limit of 10^{14} – 10^{15} n/cm². It is feasible to increase this limit by switching to a wide bandgap semiconductor material and raising the dopant levels.

Optical Encoding and Digitization

Optical telecommunication fibers (OTFs) were developed to specifically address concerns related to EMI-induced noise. They feature low signal dispersion, are EMI-immune, have a small footprint, and were demonstrated to be robust under extreme temperatures, high strain, and high radiation levels. However, OTFs do exhibit reduced transmission when exposed to large amounts of ionizing radiation. To that end, optical signals are encoded in time, instead of in amplitude, by using pulse-width modulation (PWM). These time-encoded pulse trains can then be

Continued on next page

Continued from previous page

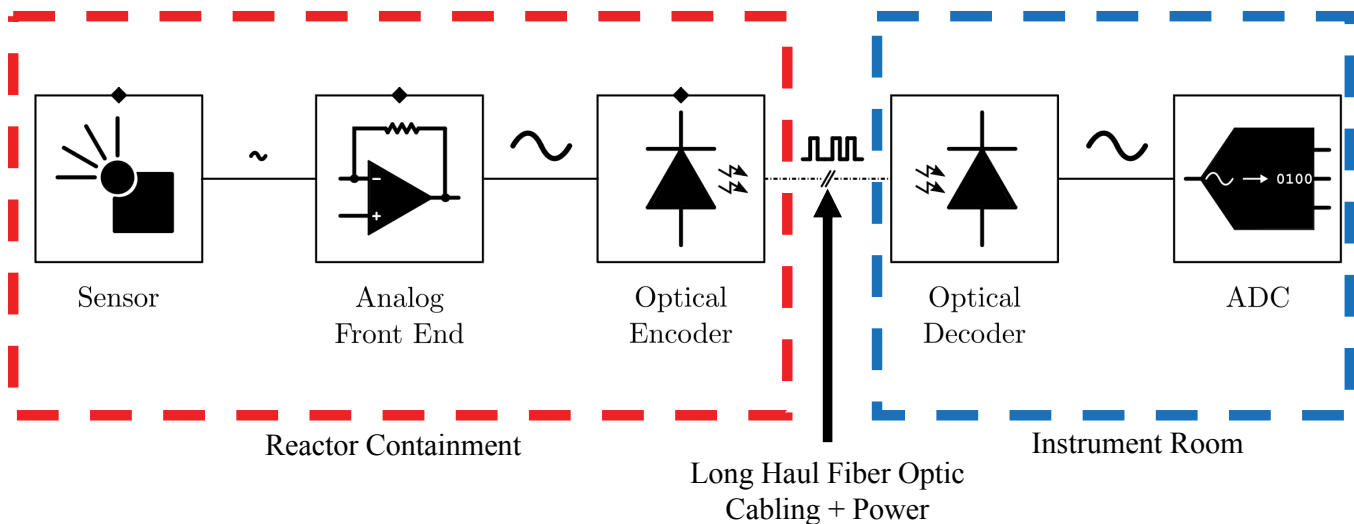


Figure 1: Block diagram of the FrEnD system. The red box indicates the portion of FrEnD inside of containment. Blue represents the portion located in a control or instrument room.

demodulated on the back end by using a low-cost, timer-based platform (e.g., a microcontroller), and the original amplitude-type signal may be reconstructed.

Using a PWM-based scheme to transmit data also serves the function of an analog-to-digital converter (i.e., digitizer) such as would typically be used to record sensor data. Because PWM encodes the relative amplitude of an input signal with a higher frequency carrier signal, such methods split data into discrete packets, with the transition between high and low levels in a pulse being proportional to the amplitude of the input signal over that time period. This is especially useful in high-radiation and other extreme environments that alter the transmissivity of optical fibers. Instead, using PWM only requires that the transition between high and low logic levels be reliably resolved.

In addition to time encoding, PWM-based encoding schemes can be readily extended to provide readouts from an array of sensors by employing methods such as time-division multiplexing (TDM). TDM, in combination with PWM, involves encoding one or more measurements from a single sensor in an array, followed by the same number of measurements from a subsequent sensor. In this manner, TDM enables an array of sensors to be interrogated using a single optical fiber. The time domain windows used in a TDM scheme must reflect the sensors' response time, but it can be easily implemented to provide updates from an array of sensors on the order of <10 ms (>100 Hz).

As of this writing, a low-cost platform utilizing microcontroller timers has been developed. Preliminary data demonstrates that this system is capable of demodulating PWM-encoded measurements transmitted via optical fiber. The circuitry required to multiplex analog electrical signals through TDM, and then encode them

for transmission by using PWM, has been simulated and prototyped on printed circuit boards to demonstrate the end-to-end feasibility of this approach, as part of the fiscal year 2022 statement of work.

Future Directions

Future plans for FrEnD include benchtop testing of the full system, using temperature sensors to provide the input. Irradiation tests to identify weak points and failure modes are also planned for fiscal year 2023, with the final test being a field test within a nuclear reactor. Finally, a second-generation FrEnD system is planned to include power harvesting and perhaps wide band-gap transistors in lieu of JFETs to increase the operational temperature and radiation hardness. Power harvesting will enable the AFE and transmission circuitry to be powered from within the reactor containment, negating any need for external power cabling. One method of in-core power generation being considered is a thermo-electric generator (TEG). The end result will be a self-powered system that requires only a single fiber optic cable passing out of the reactor containment.

This manuscript has been authored by UT-Battelle, LLC, under contract DE-AC05-00OR22725 with the US Department of Energy (DOE). The US government retains and the publisher, by accepting the article for publication, acknowledges that the US government retains a nonexclusive, paid-up, irrevocable, worldwide license to publish or reproduce the published form of this manuscript, or allow others to do so, for US government purposes. DOE will provide public access to these results of federally sponsored research in accordance with the DOE Public Access Plan (<http://energy.gov/downloads/doepublic-access-plan>).

Development of Drift Models for High-Temperature Nuclear Thermocouples

Scott Riley

Boise State University

Brian Jaques

Boise State University

Richard Skifton

Idaho National Laboratory



Motivation and Background:

New cladding, fuel, and structural materials are being developed in the pursuit of safer and more economic energy from existing nuclear reactors and Generation IV reactor designs^[1-5]. However, data on the performance of these materials at temperatures over 1200°C and neutron fluxes in the order of 10¹⁴ N/cm²s are limited^[6-12].

For the measurement of temperature, one method being evaluated is the use of thermocouples. However, traditional thermocouples (e.g., types K, N, and C) experience drift in the generated electromotive force (EMF), either due to degradation at temperatures above 1100°C, or to transmutation of the thermoelements^[6, 7, 12, 13].

To meet this design challenge, Idaho National Laboratory (INL) developed a high-temperature irradiation-resistant thermocouple (HTIR-TC) composed of commercially available phosphorus-doped niobium and lanthana-doped molybdenum thermoelements, alumina insulation, and a sheath made of either niobium or its alloys^[14]. The stability and reliability of the HTIR-TCs were investigated in a series

of out-of-pile and in-pile tests^[2, 13, 14]. In the Advanced Gas Reactor 5/6/7 (AGR 5/6/7) test, HTIR-TCs were placed within INL's Advanced Test Reactor for a total of 125 effective full-power days^[13]. **Table 1** compares HTIR-TCs against commonly used thermocouples at nuclear reactors in terms of irradiation- and temperature-caused drift under the conditions featured in the AGR 5/6/7 test.

High-Temperature Irradiation-Resistant Thermocouple Objectives:

HTIR-TCs are expected to be used in Generation IV nuclear reactors, in fuel validation tests conducted inside material test reactors, and for recording measurements during abnormal conditions during the operation of nuclear power stations. The scope of this activity is to apply an empirical model of HTIR-TC drift to other commercially available thermocouples in order to compare any differences in performance for comparison when operating in the nuclear reactor environment.

The following are the main parameters to consider when using the drift model to compare the performance of commercially available thermocouples with that of HTIR-TCs: length of exposure to high temperatures, thermal neutron flux, and fast neutron flux. Comparison of the modeled EMF signal drift for HTIR-TCs with that of type K, N, C, S, and B thermocouples will demonstrate the need for HTIR-TCs in Generation IV reactors, as well as for HTIR-TC in situ temperature measurements during accident scenarios.

The performance of HTIR-TCs is dependent on a preliminary heat treatment above the maximum service temperature. The mechanism behind stabilizing the EMF signal is not fully understood, so the experimental component of this activity is aimed at demonstrating

Thermocouple	Temperature Range (°C)	Irradiation Drift (%)	High Temperature Drift (%)
C	0 – 2315°C	-18.99	-0.22
K	-270 – 1260°C	-0.02	-0.12
N	-270 – 1260°C	-0.45	-0.66
HTIR-TC	0 – 1700°C	-0.46	Negligible

Table 1. Comparison of HTIR-TCs against traditionally used thermocouples for nuclear applications. The temperature- and irradiation-caused drifts were determined for a temperature of 1083°C and a neutron fluence of 1.8x10²¹ N/cm²^[6, 7, 12, 13].

Continued on next page

Continued from previous page

a mechanistic understanding of HTIR-TC stabilization and performance. A preliminary understanding of the stabilization heat treatment was conducted to force interactions between thermoelements (Mo and Nb), as well as the alumina insulation, to reduce HTIR-TC drift over time at elevated temperatures. Several insulators were explored, and with alumina currently considered as the best choice due to its desirable properties and stability.

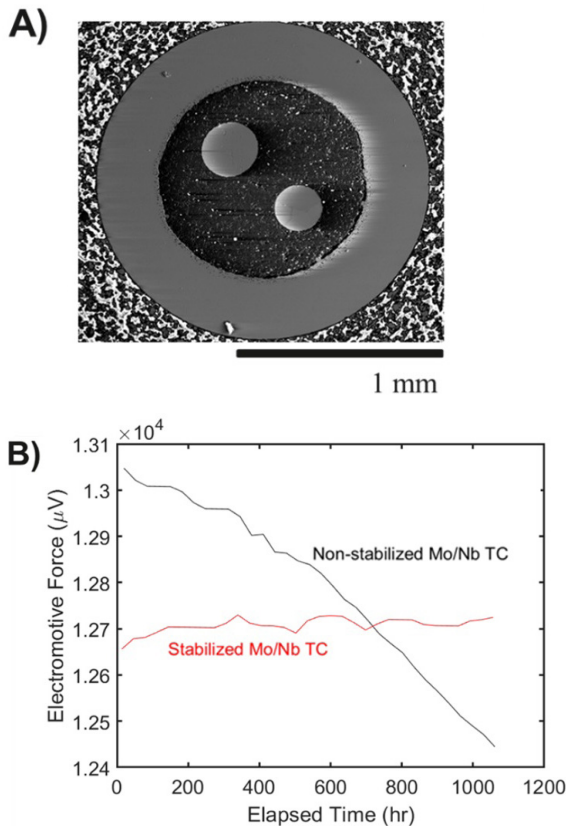


Figure 1. (A) Scanning electron micrograph of a HTIR-TC cross section after heat treatment at 1600°C for 24 hours. (B) EMF signal measured by Mo/Nb thermocouples during a 1000 hour test at 1100°C.

Current Status

Comparison against the irradiation-induced drift rates of commonly used thermocouples for temperature sensing in both irradiative and high-temperature environments was achieved using the drift model developed by Skifton (see **Figure 2**)^[13]. In this comparison, the impact of transmutation on the EMF signal of each thermocouple was determined in regard to the conditions seen during the AGR 5/6/7 test.

The irradiation-induced drift in the EMF signals of HTIR-TCs is comparable to that of Cambridge type N and type K thermocouples. Type S, B, and C thermocouples experienced a higher EMF drift rate in comparison to

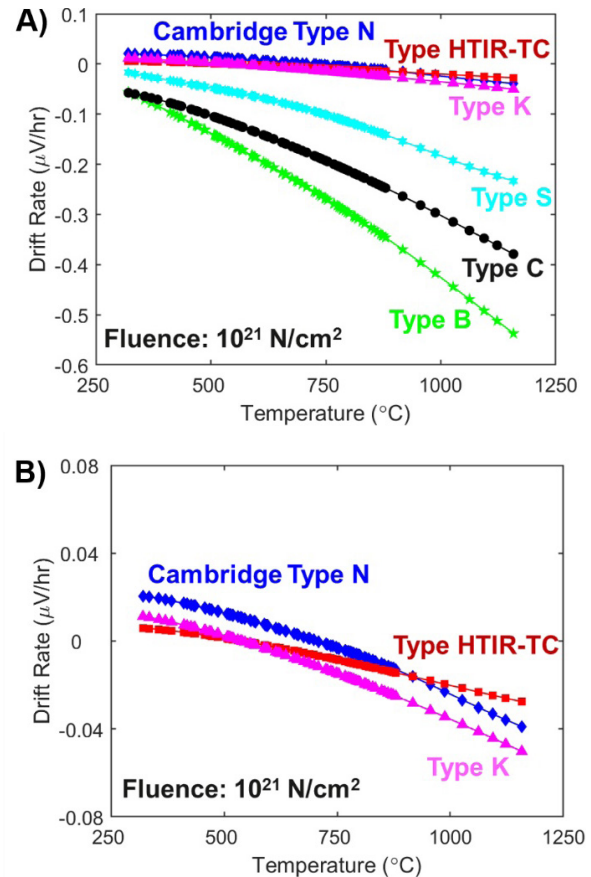


Figure 2. Irradiation-induced drift in the EMF signals of commonly used thermocouples for temperature sensing in both irradiative and high-temperature environments up to 1200°C. (A) Shows the drift range for all of the common thermocouples where as (B) shows a zoomed-in section of the reduced drift and similar behaviour of the Cambridge Type N, Type HTIR-TC, and Type K thermocouples.

HTIR-TCs. This higher drift rate is due to the rhenium and rhodium content within these thermocouples increasing the likelihood of transmutation. The comparison reveals that HTIR-TCs combine the irradiation tolerance of Cambridge type N and type K thermocouples with the high-temperature sensing capabilities of a type B thermocouple.

During the preliminary heat treatment of the HTIR-TCs, an interaction region formed between the alumina insulation and the niobium thermoelement. Diffusion of alumina into niobium has been characterized in the literature to occur at temperatures of at least 1450°C^[15]. Once heat-treated to 1450°C, the EMF signal did not vary with increasing heat treatment temperature (**Figure 3**), nor with prolonged dwells below the stabilization heat treatment temperature. Stabilization of the HTIR-TC EMF signal is dependent on the formation of an interaction region between the niobium thermoelement and the alumina insulation.

Continued on next page

Continued from previous page

Conclusion

Development of in-core instrumentation is driven by the pursuit of safer and more economic energy from both existing nuclear reactors and Generation IV reactor

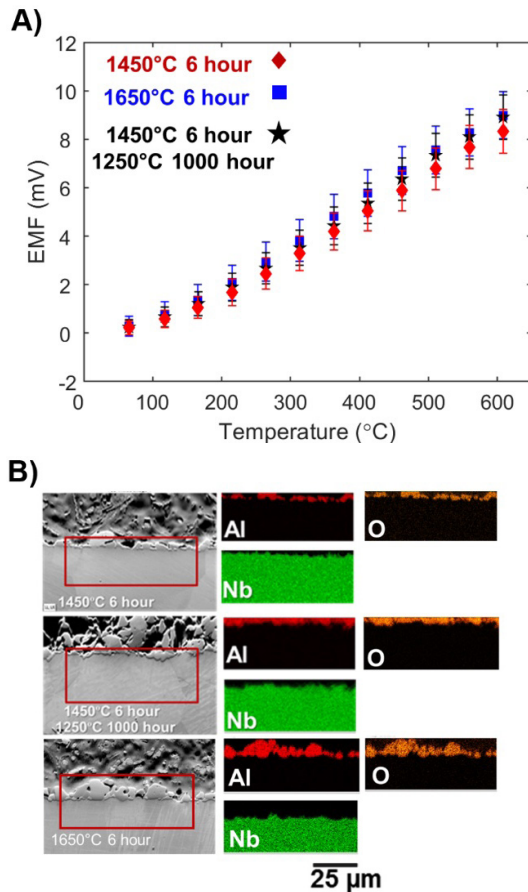


Figure 3. (A) The EMF signal did not vary with increasing stabilization heat treatment temperature. In addition, after undergoing the stabilization heat treatment, prolonged exposure to temperatures below the stabilization heat treatment temperature did not impact the EMF signal. (B) During the stabilization heat treatment, an interaction region developed between the Nb-P thermoelement and the alumina insulation.

designs. With increasing reactor temperatures, efficiency can be increased, reducing the cost of energy production. However, the safety of these reactors is dependent on the margin between the operating temperature and temperatures for which the probability of fuel failure is high. These safety margins are based on the uncertainty factor of the fuel temperature measurement. The ability to measure reliable temperature data will reduce this uncertainty factor and permit reactor operations at higher temperatures.

HTIR-TCs combine the high-temperature sensing capabilities of type B thermocouples with the irradiation tolerance of type K and N thermocouples. HTIR-TCs will

enable reliable fuel temperature sensing at temperatures above 1200°C and neutron fluxes on the order of 10^{14} N/cm²s. Commercialization of HTIR-TCs will help reduce the economic cost of energy produced from nuclear power reactors, and improve safety by providing reliable in-pile temperature measurements.

References

- [1] B. G. Kim, J. L. Rempe, J. F. Villard, S. Solstad, "REVIEW OF INSTRUMENTATION FOR IRRADIATION TESTING OF NUCLEAR FUELS AND MATERIALS," Nuclear Technology, Vol. 176, No. 2, 2011, pp. 155–187.
- [2] J. L. Rempe, D. L. Knudson, K. G. Condie, J. C. Crepeau, J. E. Daw, S. C. Wilkins, "OPTIONS EXTENDING THE APPLICABILITY OF HIGH-TEMPERATURE IRRADIATION-RESISTANT THERMOCOUPLES," Nuclear Technology, Vol. 167, No. 1, 2009, pp. 169–77.
- [3] J. L. Rempe, D. L. Knudson, J. E. Daw, T. C. Unruh, B. M. Chase, K. L. Davis, et al., "Advanced In-Pile Instrumentation for Materials Testing Reactors," IEEE Transactions on Nuclear Science, Vol. 61, no. 4, 2014, pp. 1984–94.
- [4] G. S. Was, D. Petti, S. Ukai, S. Zinkle, "Materials for future nuclear energy systems," Journal of Nuclear Materials, Vol. 527, No. 3, 2019, p. 151837.
- [5] S. J. Zinkle, K. A. Terrani, L. L. Snead, "Motivation for utilizing new high-performance advanced materials in nuclear energy systems," Current Opinion in Solid State and Materials Science, Vol. 20, No. 6, 2016, pp. 401–10.
- [6] M. J. Kelly, W. W. Johnston, and C. D. Baumann, "The Effects of Nuclear Radiation on Thermocouples," Temperature Its Measurement and Control in Science and Industry, Vol. 3, 1960.
- [7] N. L. Sandefur, J. S. Steibel, and R. J. Grenda, "Emf drift of chromel/alumel and W3%/W25%Re thermocouples measured in pile to high neutron exposures," Trans Amer Nucl Soc, Vol. 16, 1973, p. 111.
- [8] M. Scervini, "Development of Low-Drift Nickel-Based Thermocouples for High-Temperature Applications," ASME, Journal of Engineering for Gas Turbines and Power-Transactions, Vol. 138, No. 8, 2016, p. 081601.
- [9] J. Machin, D. Tucker, J. Pearce, "A Comprehensive Survey of Reported Thermocouple Drift Rates Since 1972," International Journal of Thermophysics, Vol. 42, No. 10, 2021, p. 32.
- [10] M. A. Futterer, E. D'Agata, M. Laurie, A. Marmier, F. Scaffidi-Argentina, P. Raison, et al., "Next generation fuel irradiation capability in the High Flux Reactor Petten," Journal of Nuclear Materials, Vol. 392, No. 2, 2009, pp. 184–191.
- [11] M. Laurie, S. Fourrez, M. A. Futterer, J. M. Lapetite, M. Sadli, R. Morice, and G. Failliau, "Long term out-of-pile thermocouple tests in conditions representative for nuclear gas-cooled high-temperature reactors," Nuclear Engineering and Design, Vol. 271, 2014, pp. 283–290.
- [12] R. Van Nieuwenhove, L. Vermeeren, "Irradiation effects on temperature sensors for ITER application," Review of scientific instruments, Vol. 75, No. 1, 2004, pp. 75–83.
- [13] R. Skifton, "High-Temperature Irradiation-Resistant Thermocouple Qualification Test Results Report," INL/EXT-21-63346, Rev. 001, Idaho National Laboratory, 2021.
- [14] J. L. Rempe, D. L. Knudson, K. G. Condie, and S. C. Wilkins, "Thermocouples for high-temperature in-pile testing," Nuclear Technology, Vol. 156, No. 3, 2006, pp. 320–331.
- [15] M. Ruhle and A. G. Evans, "Structure and chemistry of metal/ceramic interfaces," Materials Science and Engineering: A, Vol. 107, 1989, pp. 187–197.

A Liquid Metal Laser Ultrasound Transmitter for High-Temperature NDT

Nicholas Garcia

North Carolina State University

Ho-Wuk Kim

North Carolina State University

Sean Kerrigan

North Carolina State University

Geet Khatri

North Carolina State University

Mo-Yuen Chow

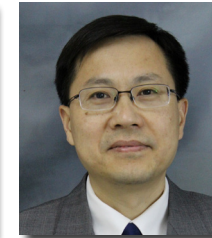
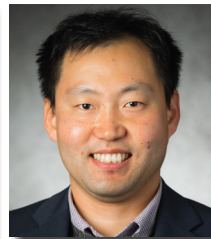
North Carolina State University

Mohamed Bourham

North Carolina State University

Xiaoning Jiang

North Carolina State University



Introduction

Today's nuclear power plants feature a complex network of sensors that monitor critical system aspects such as pressure, vibration, temperature, liquid flow, liquid level, neutron flux, and radiation levels. Designers of next-generation reactors are developing an improved sensor network to enable real-time monitoring of the structural integrity of reactors as they increase in sophistication and interconnectedness. A significant challenge to overcome in implementing these sensors is the extreme environment of plant reactor compartments. Temperatures exceeding hundreds of degrees Celsius, as well as high radiation levels from the core and coolant lines, may, over time, significantly damage sensors embedded in the structure.

This project aims to demonstrate a type of semi-invasive sensor that may be more easily maintained and can withstand the extreme temperatures and radiation levels of operating reactor compartments. Reactor maintenance operations require temporary shutdown of the entire plant, and extensive care is taken to keep personnel safe and reduce their exposure to radiation in the reactor compartment. Therefore, the benefits afforded by semi-invasive sensors include (1) reduced maintenance time, (2) increased safety and accessibility for servicing by plant personnel, and (3) reduced cost of time and resources used during maintenance. Aluminum nitride (AlN) single crystals were selected as the piezoelectric materials, as our high-temperature sensors had to overcome the extreme environmental challenges of reactor compartments^[1]. Previously, our lab had demonstrated their usefulness in measuring ultrasound at high temperatures for various structural health monitoring applications^[2,3].

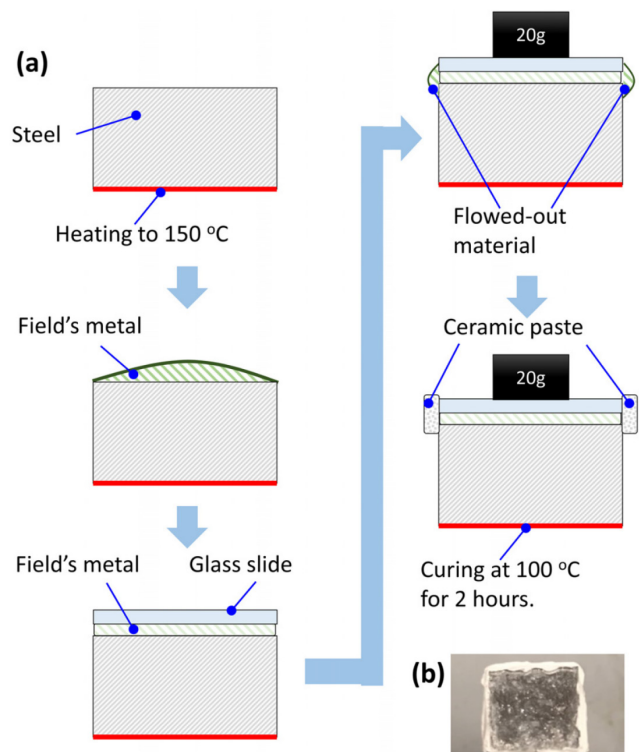


Figure 1: Step-by-step process of fabricating LM transducer.

Current Status

In 2020 and 2021, the project was impacted by COVID-19-related lab restrictions, supply chain setbacks, and personnel changes. We are working to complete the final milestones regarding sensor mockup and wireless communication system testing under a no-cost extension

Continued on next page

Continued from previous page

of this project. These milestones will combine the sensor and wireless network designs into a single platform. In this article, we briefly discuss recent accomplishments as well as the path forward.

Liquid metal transmitter: Our lab designed a high-temperature ultrasound transmitter that (1) can withstand high temperatures (>400°C), (2) generates stronger acoustic signals than when using laser ultrasound alone (no liquid metal interface, and the laser beam is directly applied to the surface of the structure), and (3) may be remotely powered by the laser. The liquid metal transducer was constructed out of Fields metal, a non-toxic metal that is liquid at 65°C (Figure 1). Heat is constantly applied to maintain the metal in a liquid state. A thin layer of the metal was placed under a glass window, and a weight was used to press the liquid metal into a flat, uniform layer. It was then sealed underneath the window by using ceramic paste. Crucial to the design was the selection of the specific liquid metal type from among the several options available. Mercury and gallium are widely known forms of liquid metal that feature room-temperature applications, but neither was chosen as the transmitter.

A thin layer (~125 μm) of a non-toxic Fields metal alloy (32.5% bismuth – 51% indium – 16.5% tin) was used, due to its significant coefficient of volumetric thermal expansion (285 ppm/K)^[4]. This parameter makes it especially useful, since the primary mechanism of ultrasound generation is the photoacoustic effect (Figure 2), which refers to ultrasound generation via a material's absorption of light and subsequent conversion to thermal expansion^[5].

The transducer is powered by the laser, and the AIN sensor is connected to a receiver that displays its output on an oscilloscope (Figure 3). Using the oscilloscope, the acoustic

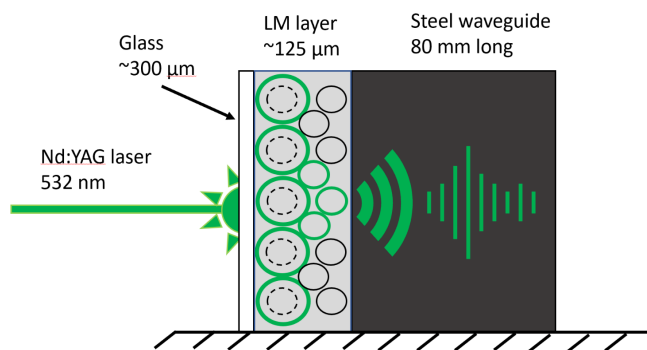


Figure 2: Liquid metal (LM) laser ultrasound transducer generating ultrasound by means of the photoacoustic effect.

data were captured and then later processed. The results showed that a liquid metal transducer could produce a readable signal at up to at least 450°C (Figure 4). The reference signal in the figure refers to the generation of laser ultrasound on a steel bar, using only the glass window

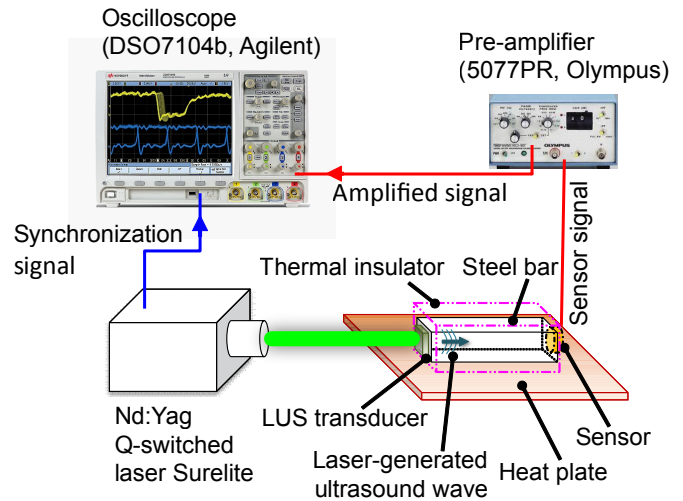


Figure 3: Experimental setup for the liquid metal laser ultrasound transducer tests.

and no liquid metal layer. Overall, we concluded that the liquid metal layer was able to produce ultrasound 30 dB than laser ultrasound on a bare metal surface alone.

Liquid metal damage detection: A liquid metal transmitter may be placed on a thin beam and activated by the laser (Figure 5). Our lab measured the acoustic signals

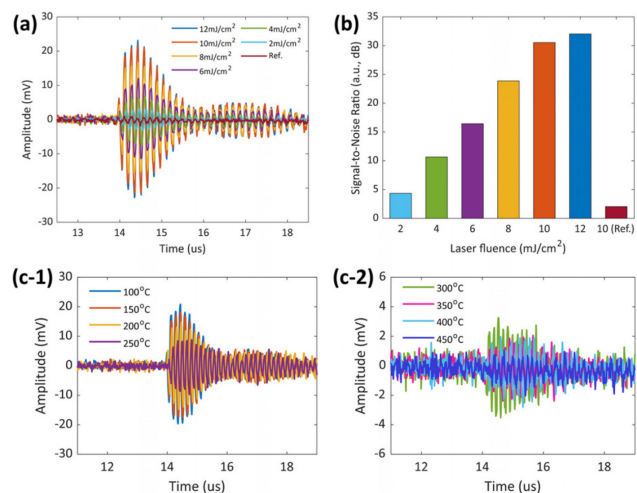


Figure 4: Results for liquid metal laser ultrasound transducer a) acoustic signal varied with degrees of laser fluence, b) Signal-to-noise ratio of the laser ultrasound with varied degrees of laser fluence, c-1) and c-2) acoustic signal amplitudes in mV with varying temperatures of the steel waveguide.

propagating through the beam and reflecting off an artificial defect. This test was conducted using a cylindrical furnace to apply a high-temperature condition to the beam from room temperature up to 1000°C. The liquid metal transmitter and the defect were left exposed to room temperature, but the AIN receiver was allowed to remain

Continued on next page

Continued from previous page

in the furnace, with a metallic heat shield clamped over it. The AlN piezoelectric sensor was able to both receive the acoustic signals from the defect as well as maintain its sensitivity in high temperatures. As the heat increases, the steel beam experiences thermal expansion, affecting the arrival time of the acoustic signal to the sensor. Once the signals were collected, the distance from the receiver to the

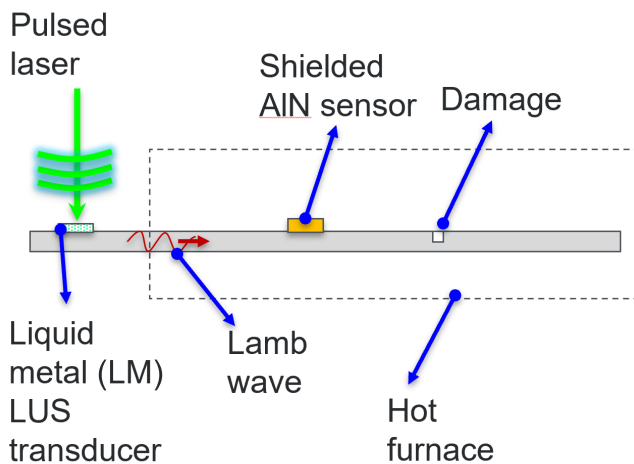


Figure 5: Diagram of the experimental setup for the damage detection in a 3 mm thick steel beam with shielded AlN Receiver.

defect was determined. However, the high-temperature condition and thermal expansion caused a discrepancy between the calculations of the predicted distance and the actual distance. Thus, we applied a correction factor to reduce the error in all the distance calculations to under 5.00%.

Wireless Data Transfer: The wireless communication system utilizes an analog-to-digital converter to capture the ultrasound signals, along with an Arduino to receive those digital signals and relay them to a Raspberry Pi. The data are ultimately displayed on a LabVIEW interface. While we had previously demonstrated its effectiveness in vibration sensing, recently we focused on improving the feature extraction. Transmission of the large amounts of data collected by the sensors is accomplished by compressing the wavelet data, sending it across a network, then reconstructing it to an acceptable level of quality while reducing the root mean square error. These are the steps that must be taken to send the enormous quantities of data gathered by the sensors. Before reconstructing the wavelets, a threshold value is selected, and any wavelets below that threshold are rejected as noise. This reduces the reconstruction time and complexity but ensures an acceptable level of quality in the final wave reconstruction. Using a steel waveguide and an AlN sensor, test pulse-echo signals were used to reconstruct wave signals, and a threshold of 1.1 was selected.

Conclusions

Based on our results, we conclude that the Fields metal layer is a useful alternative to laser-generated ultrasound for high-temperature applications. However, the liquid metal transducer is still in the early stages of development, and several paths toward improvement are worth exploring. For the remainder of this project, we intend to use the mockup platform to incorporate several designs, including liquid level sensing, damage detection sensing, and vibration sensing. We also intend to expand on the results we collected from the damage detection case, and explore 1-D defect location and size detection in a 3-mm-thick steel beam.

References

- [1] X. Jiang, K. Kim, S. Zhang, J. Johnson, and G. Salazar, "High-Temperature Piezoelectric Sensing," *Sensors*, Vol. 14, No. 1, 2014, pp. 144–169.
- [2] H. Kim, S. Kerrigan, M. Bourham, and X. Jiang, "AlN single crystal accelerometer for nuclear power plants," *IEEE Transactions on Industrial Electronics*, Vol. 68, No. 6, 2021, pp. 5346–5354.
- [3] H. Kim, "Design, Prototyping, and Validation of Noninvasive Sensors for Nuclear Power Plant Applications," Dissertation, North Carolina State University, 2020.
- [4] H. Kim, K. Kim, N. Garcia, T. Fang, and X. Jiang, "Liquid metallic laser ultrasound transducer for high-temperature applications," *Applied Physics Letters*, Vol. 118, No. 18, 2021, 183502.
- [5] F. A. McDonald and G. Wetsel, Jr., "Generalized theory of the photoacoustic effect," *Journal of Applied Physics*, Vol. 49, No. 4, 1978, pp. 2313–2322.

Printed High-Temperature Irradiation-Resistant Thermocouples for Real-Time Monitoring of Nuclear Reactor Components

Richard Fink

Applied Nanotech Inc.

Josh Eixenberger

Boise State University

David Estrada

Boise State University and
Idaho National Laboratory



Background

Additive manufacturing (AM) of sensors capable of real time monitoring of the thermal properties of nuclear reactor components is crucial for furthering the advancement of existing and next-generation nuclear reactors. Sensors employed to measure in-pile thermal properties must be able to withstand the harsh nuclear environments of high-temperature and high-neutron-flux environments while still maintaining long-term stability. Existing commercial high-temperature thermocouple elements have large neutron cross sections and transmute to other elements, leading to loss of thermocouple calibration in high-neutron-flux environments. Thermocouples fabricated using niobium (Nb) and molybdenum (Mo) have shown good resistance to this extreme type of environment but can be difficult to fabricate via traditional methods. Idaho National Laboratory developed wire-based Mo and Nb thermocouples that exhibit high-temperature, high-irradiance stability^[1, 2]. Both Mo and Nb are high-temperature refractory materials with low thermal and fast neutron cross sections, and are thus more stable than other common thermocouple materials exposed to reactor core environments. Furthermore, Mo isotopes Mo-94 through Mo-98 are stable, and most transmute into other stable Mo isotopes. Thus, the chemistry undergoes little change. Nb has a smaller thermal neutron capture cross section, and the decay paths of unstable Nb isotopes with excess neutrons lead to Mo isotopes Mo-95 and Mo-96. The Mo/Nb thermocouple sensors are applicable to all reactor designs, but the greatest need is for next-generation and metal- or gas-cooled fast reactors, in which the fuel temperature runs hotter than in current water-cooled reactor designs.

Approach

AM approaches for fabricating these high-temperature irradiation-resistant thermocouples enable fast, high-precision sensor fabrication and can be printed on conformal surfaces to monitor various structural

components at a compact size to minimize intrusion and allows for design flexibility. In this work, we developed Mo/Nb nanoparticle-based inks compatible with aerosol jet and inkjet printer technologies. We investigated the printed devices' sintering conditions and electrical properties, and now report on the printed thermocouples' performance at high temperatures. This work demonstrates the feasibility of this approach, enabling a suitable option for temperature detection in extreme environments. Although the immediate application is for temperature measurement, our technology can be used to realize alternative circuit designs for measuring strain, heat flow, and other physical parameters in a nuclear reactor core.

Initial Results

We used Mo and Nb nanoparticles to create inks that

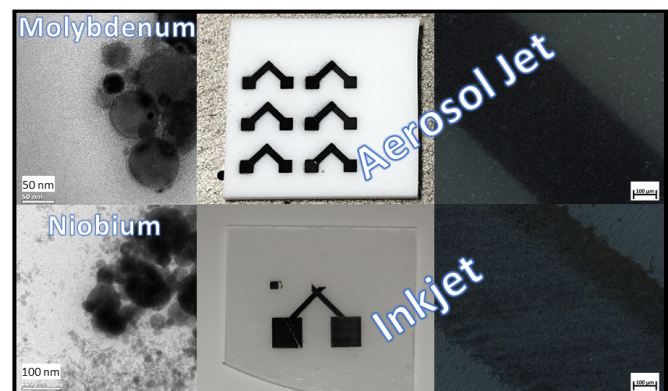


Figure 1: SEM images of Mo and Nb particles (left). Aerosol jet and inkjet printed Mo+Nb thermocouples (center & right) on Al₂O₃ substrates. The contact pads are 2mm x 2mm.

were then demonstrated in aerosol jet and inkjet printing platforms. For screen printing and dispensing applications in ceramic 3-D structures, we also made a paste formulation featuring a viscosity of 20,000 cPs.

Inkjet and aerosol jet thermocouples were printed at BSU, using both ANI and BSU inks (**Figure 1**). In parallel, ANI used both Mo and Nb inks to fill commercial ceramic



Figure 2: Diagram of ceramic tube with channels in the tube containing Mo (green) and Nb (red) ink. The inks overlap at one end to form a junction. It is important to note that

Continued on next page

Continued from previous page

thermocouple tube channels, and made a functional thermocouple by letting the ink meet at one end and then curing the inks inside the tube (**Figure 2**), a process that can be scaled up by using ceramic tubes several feet in length. Thermocouple ceramic tubing comes in a variety of dimensions, with multiple (four or more) channels affording the potential for multiple or redundant thermocouple probes.

The printed Mo and Nb patterns were successfully converted into metallic circuits via thermal processing in inert gas or hydrogen-reducing gas. Firing at near 1100°C increased the electrical conductivity of Mo and produced films with a metal luster appearance. Future collaborations with Idaho National Laboratory could expand our testing to the 1500–1600°C final operating range. The fact that both metals oxidize at high temperatures in air means that, for many applications, the circuits will need to be hermetically sealed, as is the case with the current wired-based sensors.

The thermocouple response was measured to be less than expected, as compared to wire-based thermocouples, either due to incomplete sintering of the printed Mo and Nb circuit and/or interfering EMF from poorly compensated leads. Nonetheless, our preliminary data highlight a development path for Mo/Nb HTIR fabricated using AM techniques.

Summary

We demonstrated the feasibility of formulating Mo/Nb ink and paste materials for the AM of thermal and mechanical sensors to be used in in-pile applications. Future efforts will focus on improving the thermocouple response, as well as demonstrating heat flux and capacitive strain sensor for high-temperature, high-neutron-flux environments.

Acknowledgements

This material is based on work supported by the U.S. Department of Energy, Office of Science, Office of Nuclear Energy under Award Number DE-SC0020899.

References

- [1] J. L. Rempe, D. L. Knudson, K. G. Condie, and S. C. Wilkins, "Thermocouples for High-Temperature In-Pile Testing," *Nuclear Technology*, Vol. 156, No.3, 2006, pp. 320–331.
- [2] R. Skifton, "High-Temperature Irradiation-Resistant Thermocouples," *ASI Newsletter*, Issue 12, 2020.

Additive Manufactured Strain Gauges for Structural Health Monitoring

Timothy L. Phero

Idaho National Laboratory

Michael D. McMurtrey

Idaho National Laboratory

Introduction

Monitoring strain within the hostile conditions of nuclear reactors is of interest in regard to measuring the deformation and vibrations of fuel elements and structural components during reactor power cycles (*Figure 1a*). Traditionally, resistive strain gauges (RSG) have been used for this purpose, since they are well established and enable active measurement of strain at strategic locations on a given component^[1]. RSGs, however, are confined to wired interconnections and require non-trivial attachment strategies (e.g., welding or epoxy) that may not only affect the underlying component, but also cause variable sensing performance. Successful deployment of reliable strain gauges in reactor conditions stands to benefit from improved sensor design and manufacturing techniques that allow for wider application within the vast nuclear test space (i.e., environment, sample geometry, and materials compatibility) and are necessary for qualifying and demonstrating next-generation reactor designs and materials throughout the next decade.

Methodology

The interdigitated (IDE) capacitive strain gauge (CSG) is a viable sensor design proven to offer a low profile, low hysteresis, high-strain sensitivity, and wireless sensing integration capabilities^[2,3] that would benefit nuclear



sensing applications. The current inability to purchase CSGs drives the need for direct-write additive manufacturing (AM) technologies in order to quickly fabricate IDE CSGs and offset the geometric and material-related limitations of traditional fabrication techniques. In recent years, AM has demonstrated the capability to fabricate sensors that can overcome the high-temperature environments (i.e., above 300°C^[4]) and non-planar geometric challenges (i.e., cylindrical geometries^[5]) commonly found in nuclear reactors. In addition to allowing the deposition of feature whose sizes are measured at the sub-micron level, the flexibility of AM makes it compatible with tailorable, nuclear-relevant ink materials^[6], making it an ideal tool for the rapid prototyping of miniaturized strain gauges for in-pile applications^[7].

Objectives

The objective of this initial work was to:

1. **Qualify sensor design and manufacturing:** Demonstrate and optimize the AM process to fabricate IDE CSGs that are reproducible (i.e., a similar gauge factor across multiple samples) and predictable (i.e., correlates to analytical models) in performance.
2. **Compare strain sensor technologies:** Compare the performance of the printed IDE CSGs against that of commercially available bondable free-filament RSGs. Bondable free-filament RSGs are an ideal candidate sensor for comparison purposes, as they are relatively cheap, have a small profile, and are useful for high-temperature strain measurements conducted on small substrates under laboratory conditions^[8].

The mechanical and thermal performance of the strain gauges were qualified at moderate temperatures of 20–300°C by using standardized testing procedures to simulate the temperatures found in existing light-

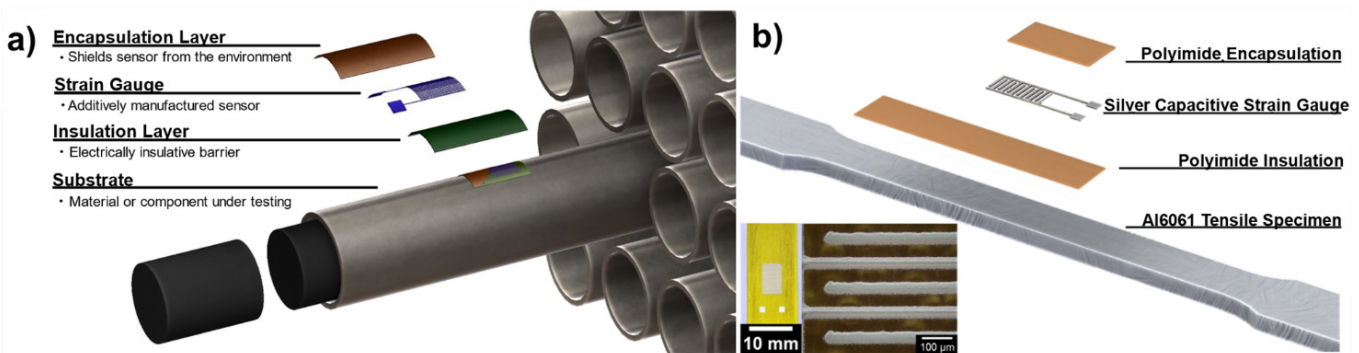


Figure 1. Schematic of an interdigitated capacitive strain gauge on (a) a fuel pin and (b) the aluminum alloy 6061 tensile specimen presently being studied. The future direction will aim to use materials less susceptible to degradation and damage caused by nuclear environments.

Continued on next page

Continued from previous page

water reactors. The results from this work will lead to the development of AM-fabricated in-pile strain gauges designed for high temperatures (i.e., 300–950°C) as well as other environmental factors found in Generation IV reactor designs.

Current Status

The additive manufactured IDE CSGs were initially fabricated and tested at Boise State University, with polyimide insulation/encapsulation and silver electrodes on a flat Al6061 substrate (**Figure 1b**). In its current state, the CSG is not ready for nuclear applications; however, this work demonstrates that the additive manufactured strain gauges, when compared to bondable high-temperature RSGs, showed promising performance for elevated temperature applications. The additive manufactured IDE CSGs closely followed the analytical models and exhibited similar strain sensitivities (e.g., gauge factor) across multiple fabricated sensors (**Figure 2**). The IDE CSG in this work also filled a knowledge gap pertaining to IDE CSGs tested at elevated temperatures (i.e., above 100°C) on metallic substrates and in low-strain environments (i.e., $\approx 1000 \mu\epsilon$) prototypic of nuclear applications. Demonstrating reproducible and predictable strain-sensing performance are two important factors when deploying these strain gauges in costly, time-consuming experiments (e.g., test reactor facilities).

Path Forward

Application of additive manufactured sensors in harsh environments requires careful selection of materials, along with improved strategies in terms of both packaging and heterogenous integration. Presently, efforts are underway to investigate the fabrication of IDE CSGs composed solely of metal and ceramic constituent layers (**Figure 1**) that are less susceptible to damage and degradation. This is supported by Idaho National Laboratory's current capability to develop and optimize AM ink materials that are application-specific for the printed device. The additive manufactured IDE CSGs will also continue to be exposed to separate effects testing (e.g., mechanical strain, temperature, and vibration), and used to support nuclear programs in which current RSG technologies are inapplicable due to size constraints. Although not currently within the scope of our project, it is recognized that successful CSG deployment also requires significant improvements in signal processing and data acquisition to enable stable, long-term CSG measurements with intrinsic balancing, error compensations, and minimal circuit drifting.

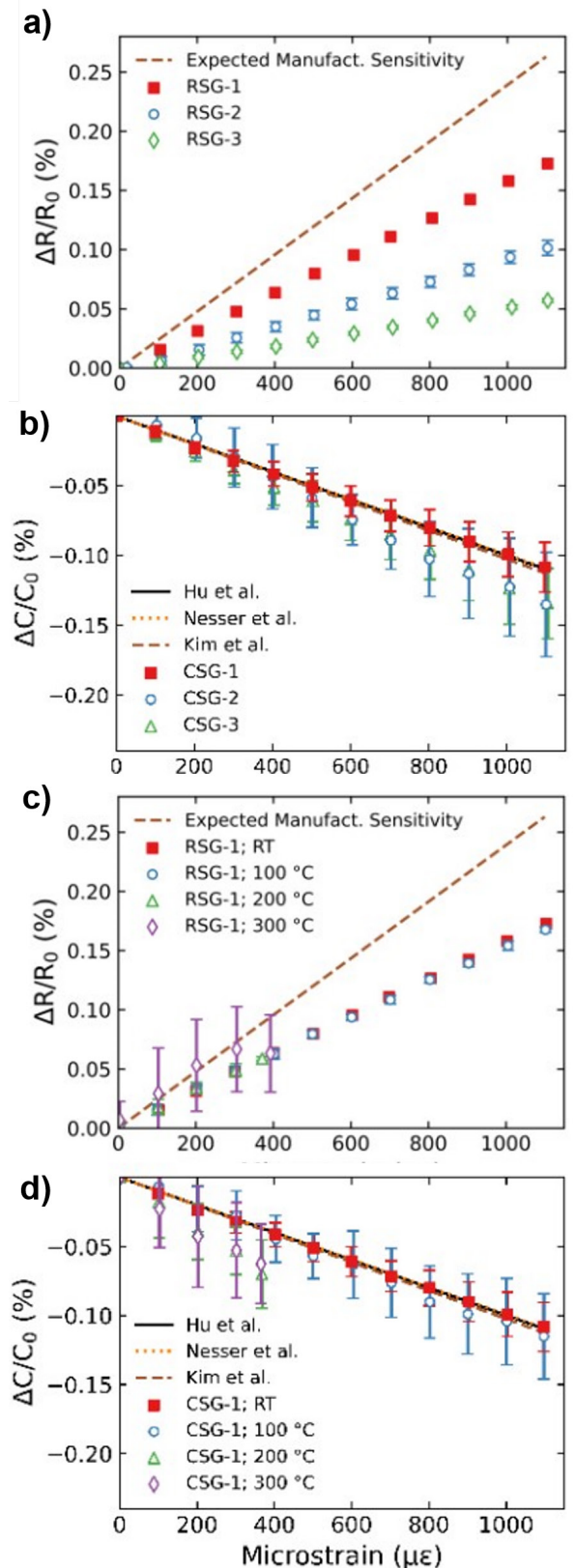


Figure 2. Testing results of the commercial resistive strain gauges at (a) RT and (c) elevated temperature, and printed strain gauges at (b) RT and (d) elevated temperature.

Continued on next page

Continued from previous page

Conclusion

In this work, AM was used to fabricate low-profile IDE CSGs that are reproducible and also predictable in terms of strain-sensing performance. These efforts support other U.S. Department of Energy, Office of Nuclear Energy programs (e.g., the Advanced Reactors Technologies and Advanced Materials and Manufacturing Technologies programs) through the implementation of advanced manufacturing techniques in fabricating sensors that enable data acquisition for improved material testing, and that aid in validating modeling and simulation efforts to support the development, testing, and qualification of new nuclear materials.

References

- [1] M. J. Pettigrew, "The behaviour of weldable strain gauges under nuclear reactor core conditions," *Nuclear Engineering and Design*, Vol. 263, 2013, pp. 350–361.
- [2] S. R. Kim, J. H. Kim, and J. W. Park, "Wearable and Transparent Capacitive Strain Sensor with High Sensitivity Based on Patterned Ag Nanowire Networks," *ACS Applied Materials & Interfaces*, Vol. 9, No. 31, 2017, pp. 26407–26416.
- [3] H. Nesser, J. Grisolia, T. Alnasser, B. Viallet, and L. Ressler, "Towards wireless highly sensitive capacitive strain sensors based on gold colloidal nanoparticles," *Nanoscale*, Vol. 10, No. 22, 2018, pp. 10479–10487.
- [4] M. T. Rahman, R. Moser, H. M. Zbib, C. V. Ramana, and R. Panat, "3D printed high performance strain sensors for high temperature applications," *Journal of Applied Physics*, Vol. 123, No. 2, 2018, pp. 1–12.
- [5] S. Vella, C. Smithson, K. Halfyard, E. Shen, and M. Chrétien, "Integrated capacitive sensor devices aerosol jet printed on 3D objects," *Flexible and Printed Electronics*, Vol. 4, No. 4, 2019, pp. 1–16.
- [6] K. T. Fujimoto, et al., "Additive Manufacturing of Miniaturized Peak Temperature Monitors for In-Pile Applications," *Sensors*, Vol. 21, No. 22, 2021, p. 7688.
- [7] T. L. Phero, et al., "Additively manufactured strain sensors for in-pile applications," *Sensors and Actuators A: Physical*, 2022, p. 113691.

Techno-Economic Assessment of a Multi-Band Heterogenous Wireless Network Architecture for Nuclear Power Plants

Koushik A. Manjunatha
Idaho National Laboratory

Vivek Agarwal
Idaho National Laboratory



one-size-fits-all solution. In addition, wireless technologies vary according to application, service area, service set, and economic conditions. To address these technical and economic requirements, this research developed a multi-band heterogeneous wireless network architecture and performed a techno-economic analysis (TEA) of the network for define scenarios.

Introduction

Nuclear power plants (NPPs) are utilizing technological advancements to automate monitoring, inspection, security, and other operation and maintenance tasks, thus improving the operating efficiency and economic competitiveness of NPPs without compromising safety or reliability. One technology currently enabling automation and significant cost reductions is wireless communication. Although wired solutions represent reliable channels for transmitting data, wired network deployment costs are extremely high. The

TEA is a type of modeling that examines research and development areas in terms of technological feasibility, cost, benefits, and risks and uncertainties. This helps businesses better understand the factors involved in bringing a given project to fruition^[1].

Network Architecture

The multi-band heterogeneous wireless network architecture (see *Figure 1*) is predominantly driven by a distributed antenna system (DAS) or wireless local area network (WLAN) system. In a DAS system, the entire coverage area is divided into smaller regions, each connected to a DAS backhaul via fiber optic cables.

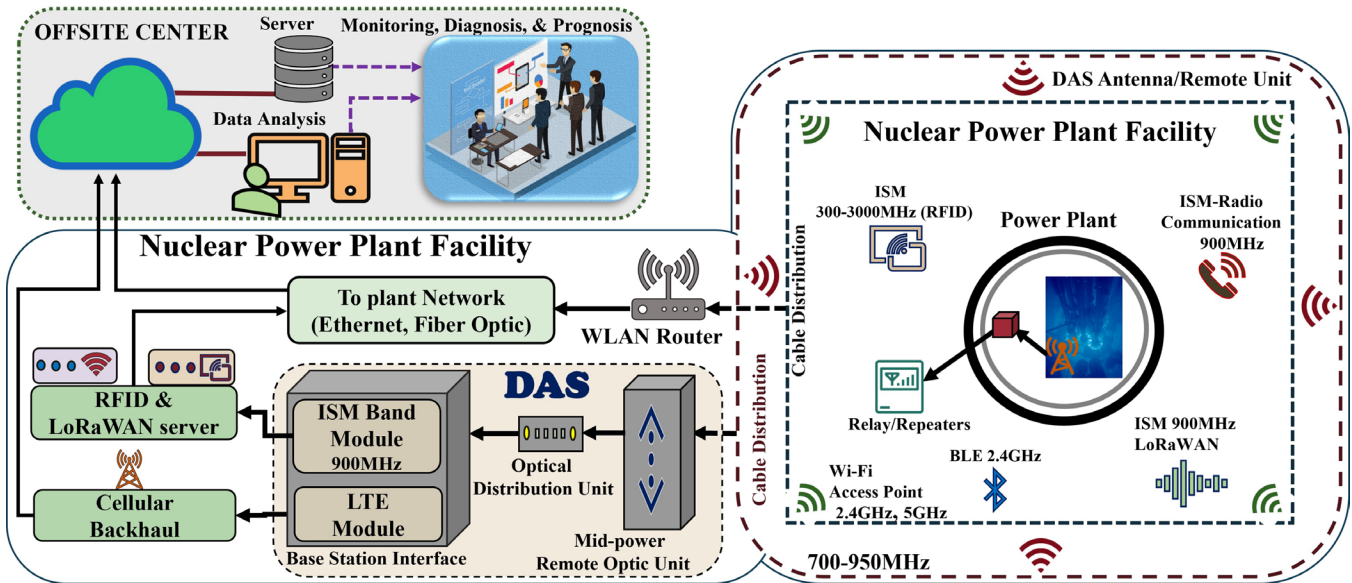


Figure 1. Envisioned wireless network architecture for NPP automation.

emergence of fifth-generation (5G) wireless technology, along with several advanced low-power Internet of Things technologies, has initiated a paradigm shift in industrial automation.

NPP-related applications entail a wide array of requirements, ranging from low- to high-power, low- to high-frequency, and short- to long-range communications. This presents a challenge, as there is no

Dividing the coverage area into smaller regions enhances performance in terms of path loss and transmission power. A DAS does not generate a signal; instead, the signal from the base station (BS) is distributed to several antenna units via coaxial or fiber optic cables installed in and around the NPP site. DAS networks are typically used to accommodate carrier-based cellular networks in indoor environments.

Continued from previous page

Alternatively, a WLAN system offers a high-data-rate internet connection and is comprised of low-coverage, limited-capacity access points (APs) operating at an unlicensed spectrum of 2.4 and 5 GHz. To fulfill the coverage and capacity requirements, the WLAN system provides network capacity by distributing limited frequency wireless APs around the monitoring area.

Most wireless technologies operate in an unlicensed industrial, scientific, and medical (ISM) band (900 MHz in North America) for low-power, low-bit-rate, and long-range applications. These technologies, along with other networks (e.g., Bluetooth Low Energy and Zigbee) and sensor modules (e.g., video surveillance or mmWave radar modules), as shown in **Figure 1**, can be integrated along with cellular technology by using a DAS-based structure.

Techno-Economic Framework

Figure 2 shows the TEA framework utilized in this research. Based on application-specific requirements for a multi-band heterogeneous wireless network architecture, technical and economic considerations were evaluated for defined scenarios (based on attenuation levels and data traffic). These technical and economic considerations included:

- A. **Wireless network capacity and coverage** are important considerations when designing and deploying any wireless network. Wireless coverage depends on the power transmission from the transmitter (e.g., cellular BS or WLAN AP) to the receiver. Wireless capacity depends on the type of communication technology and amount of spectrum (bandwidth) selected.
- B. **Total cost of ownership (TCO)** defines the total network deployment expenditures, including the cost of purchasing, operation, upgrades (direct and indirect), and maintenance over a specific period. TCO is also an effective metric for assessing the profitability of the entire network structure over its entire lifecycle by providing an estimated calculation model for each network component, based on different cost structures. TCO includes capital expenditures (CAPEX) and operational expenditures (OPEX). CAPEX encompasses initial network equipment (e.g., radio equipment, software, and security), network installation costs, network infrastructure costs (e.g., cabling), and network management costs. OPEX kicks in once the network has been deployed, is fully functional, and has been handed over to an operation and maintenance system. More specifically, OPEX includes power consumption, troubleshooting, repair services, pricing and billing costs, operational

network planning costs (e.g., day-to-day planning, optimization, and upgrades), and human resource costs such as wages and salaries.

- C. **Net Present Value (NPV)** specifies the potential return on investment for the network deployment, assuming that future cash flow values and risk-adjusted discount rates (e.g., weighted average cost of capital) are known.
- D. **Performance Analysis** assesses throughput and latency as the two primary network performance indicators for evaluating the proposed wireless network architecture. Throughput is defined as the rate of successful data transmission, while latency is

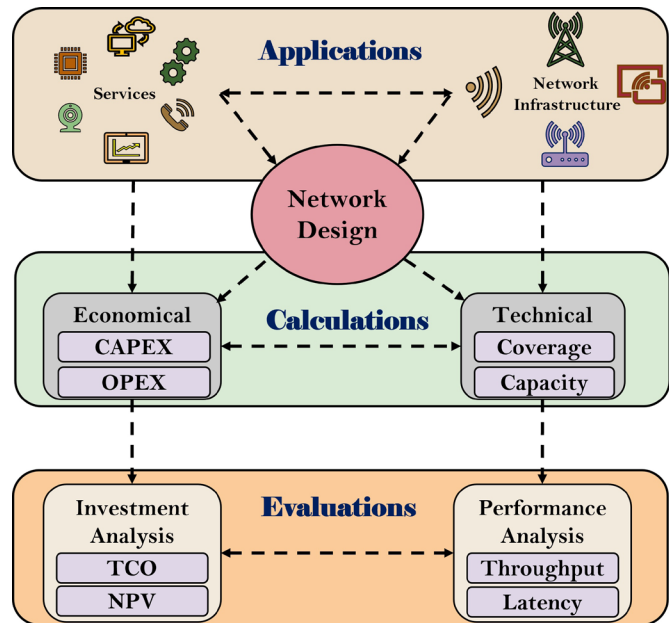


Figure 2. Flow diagram of the TEA model.

the amount of time required to transmit the data from the source to the receiver. These network performance indicators must be able to meet different application requirements under various types of operating environments.

Results

Table 1 shows the estimated CAPEX and OPEX values for a DAS network with dimensions of 100x100 m² dimension—for different attenuation levels, with and without ISM band technologies, and for a WLAN network (2.4 and 5 GHz). The estimated NPV for 5 years at a discount rate of 10% was calculated by considering an average total annual savings of \$105,000 per plant as the expected cash inflow, and the CAPEX and OPEX resulting from the wireless network deployment as the total cash outflow. In addition, the OPEX for a wireless network infrastructure was assumed

Continued on next page

Continued from previous page

Table 1. Cost analysis and technical performance results for a NPP deployments.

Cost	Signal Attenuation (dB)	DAS	DAS+ISM	WLAN 2.4 GHz	WLAN 5 GHz
CAPEX (\$K)	20	24.72	29.0	19.9	24.9
	30	31.72	35.99	23.65	32.4
	40	45.72	50.0	31.15	46.15
OPEX (\$K)	20	1.17	1.23	0.81	1.61
	30	1.68	1.74	1.41	2.82
	40	2.69	2.75	2.62	5.02
NPV (\$M)	20	0.40	0.402	0.414	0.405
	30	0.398	0.393	0.407	0.391
	40	0.379	0.374	0.394	0.367

Traffic Type	Signal Attenuation (dB)	DAS		Analysis not Performed	WLAN (2.4 and 5 GHz)	
		Throughput (Kbps)	Latency (ms)		Throughput (Kbps)	Latency (ms)
M2M	20	97.94	3.13		98.25	9.81
	30	97.87	3.12		98.18	0.14
	40	97.84	3.12		98.07	1.61
RT Video	20	932.43	136.7		1088.29	224.5
	30	923.11	149.8		701.91	5.55
	40	97.84	3.12		698.67	5.60
HD Video	20	1637.29	117.0		1828.68	772.0
	30	1384.06	135.80		852.56	147.60
	40	1132.56	164.70		802.85	164.70

to increase by 10% each year. Based on these assumptions and estimations, the calculated NPVs for the NPP under each different scenario are positive, indicating that the proposed wireless network infrastructure is expected to be profitable for the NPP.

To validate the network performance, the DAS and WLAN were simulated by using the NS3 framework, a network simulator, to mimic data traffic such as machine-to-machine (M2M), real-time (RT) video, and high-definition (HD) video for different attenuation levels (**Table 1**). For the M2M and RT video data transmissions, both the DAS and WLAN met the data rate and latency requirements. In the case of HD video, the DAS failed to meet the data rate and latency requirements, whereas the WLAN succeeded. For more details on the TEA framework and related discussions, see^[2].

Future research efforts will focus on evaluating such technical considerations as interference, co-existence of different wireless communication technologies, and the optimization of bandwidth utilization via a machine learning approach.

References

- [1] K. A. Manjunatha and V. Agarwal, "Review of Wireless Communication Technologies and Techno-Economic Analysis," Idaho National Laboratory, INL/EXT-19-53966, Idaho Falls, 2019.
- [2] K. A. Manjunatha and V. Agarwal, "Multi-Band Heterogeneous Wireless Network Architecture for Industrial Automation: A Techno-Economic Analysis," *Wireless Personal Communication*, vol. 123, pp. 3555–3573, 2022.

Design and Prototyping of Advanced Control Systems for Advanced Reactors Operating in the Future Electric Grid

R. Ponciroli

Argonne National Laboratory

A.J. Dave

Argonne National Laboratory

H. Wang

Argonne National Laboratory

T.N. Nguyen

Argonne National Laboratory

R.B. Vilim

Argonne National Laboratory

B. Kochunas

University of Michigan

A. Cilliers

Kairos Power LLC



Introduction

Nuclear power plants currently in operation are struggling to remain competitive in U.S. deregulated markets, and many premature shutdowns have occurred. One late-2018 study found that over a third of these plants are unprofitable and/or scheduled to close^[1]. One of the directions pursued by utilities consists of limiting operating and maintenance (O&M) costs generated by large site crews, physical security personnel, and extensive upkeep requirements. (Labor accounts for over 70% of non-fuel O&M costs, thus constituting the largest component of total lifecycle costs.) Though regulatory compliance is a significant driver of labor requirements, operating costs can be balanced with regulator demands. Another conclusion that can be drawn is that traditional baseload operation is not sufficiently profitable for a plant to survive in the future electric grid. Given the increasing penetration of renewable energy sources and the volatility of fossil fuel prices, one solution for renewing nuclear power's competitiveness is the enhancement of load-following capabilities. Advanced reactor designs have been identified as suitable for the new paradigm of coupling nuclear power plants with energy storage technologies.

The objective of this research is to improve the economic competitiveness of advanced reactors through the optimization of costs and plant performance. As pointed out by R. Wood, "To avoid the prospect that high staffing levels relative to unit power production will lead to unsustainable O&M costs for small reactors, a significantly higher degree of automation, to the point of near autonomy is necessary"^[2]. An architecture comprised of an automated reasoning algorithm that closely interacts

with a multi-layer advanced control system is proposed (**Figure 1**). The former provides real-time monitoring of the condition of components and engineered systems in order to minimize staffing costs and maintenance interventions. The latter allows coordination of the control procedures to

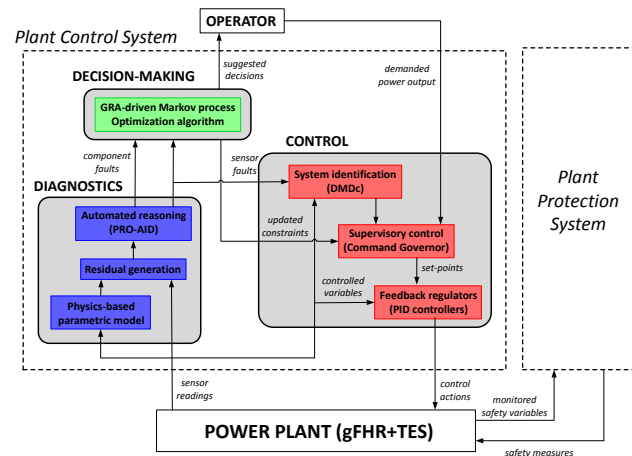


Figure 1. Structure of the proposed control system architecture.

enable autonomous operation of the plant. To build this architecture within the project's 3 year timeframe, existing in-house tools and methods developed in other Nuclear Energy Enabling Technologies (NEET) projects^[3, 4] are being leveraged, expanded, and integrated.

Continued on next page

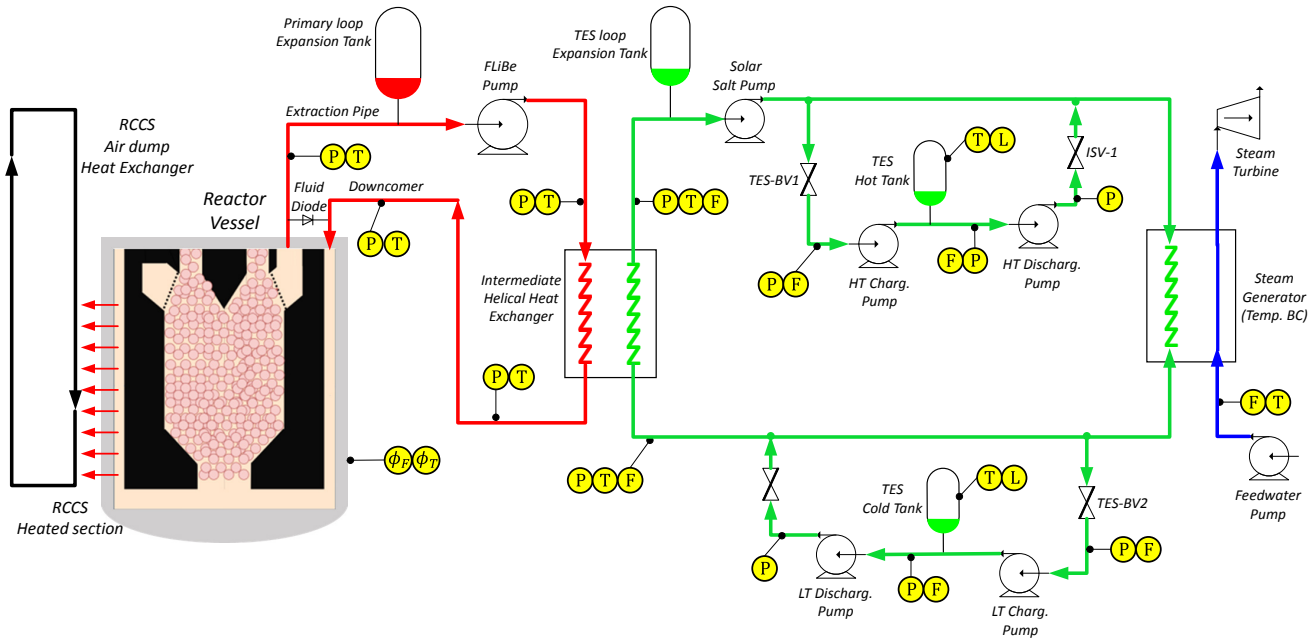


Figure 2. P&ID of the coupled system used as the test case. The primary circuit, intermediate circuit, and interface on the Rankine cycle are shown (yellow balloons represent the available sensors).

Selection of an Advanced Reactor Concept as a Test Case

Figure 2 shows the piping and instrumentation diagram (P&ID) of the integrated energy system adopted in this project. In particular, a pebble-bed, fluoride-salt-cooled high-temperature reactor (FHR) was selected. This concept uses a novel combination of existing technologies to achieve unique levels of economy, safety, flexibility, and security in nuclear power production, including pebble-type high-temperature coated tri-structural isotropic (TRISO) particle fuel and molten fluoride salt coolants. The reactor configuration selected by Kairos Power, LLC was based on the University of California, Berkeley Mark 1 design (gFHR)^[5] and serves as the reference test case. As for thermal energy storage (TES), the intermediate loop embeds two large storage tanks (a common configuration for liquid sensible heat systems), along with pumps to transport the fluid. A Rankine cycle was selected as the energy conversion system. A high-fidelity model was realized by adopting the System Analysis Module (SAM) code^[6] to both derive control/diagnostics digital twins (DTs) and to perform system-level simulations.

Major ideas behind the Autonomous operation paradigm

To achieve significant savings via the autonomous operation paradigm, plugging in a single advanced control algorithm into a state-of-the-art architecture is insufficient (main control room operations staffing is relatively small compared to overall plant staffing). Prompt detection of component and sensor performance degradation through

automated diagnostics would allow for crew sizes and equipment inspection frequencies to be reduced. Studies have estimated potential maintenance cost savings of more than \$1B over the life of GW-scale plants^[7]. Therefore, it is clear that a control system architecture that ensures autonomous operation requires a tight integration of control, diagnostics, and decision-making algorithms that can support operators in making informed choices about plant operation and maintenance interventions scheduling (Figure 1). The following are other key concepts behind the application of this paradigm to nuclear units:

- *Control- and safety-oriented priorities must remain distinct*
The Plant Control System (PCS) performs control actions to generate the electric power demanded by the operator. The Plant Protection System (PPS) is expected to trip actuators whenever monitored process variables exceed the safety limits. As shown in Figure 1, the PCS and PPS are two independent entities with very different roles.
- *Need of a diagnostics algorithm that can detect and discriminate sensor-level faults*
A major concern in adopting data-driven techniques for plant operation is the impact of uncertainties. In a world where data are forever increasing in importance, trust in available sensor readings is crucial. A diagnostics algorithm that can discriminate between sensor-level and component-level faults is necessary. Thus, the software package PRO-AID, which was

Continued from previous page

developed at Argonne National Laboratory^[4] and uses a form of automated reasoning to perform real-time monitoring and diagnostics for engineering systems, was adopted. automated reasoning is adopted.

- Limiting the complexity of the architecture*
 Integration of algorithms that perform control, diagnostics, and decision-making tasks results in multiple connections and an intense data flow. Such an unexplored level of integration generates unprecedented failure modes. For this reason, the simplest configuration possible must be adopted.

Progress and Next steps

The normal operating envelope is a concept widely used in nuclear industry to represent design-basis normal operating conditions^[8]. This expression refers to the set of limits and conditions within which the unit must operate to ensure conformance with the safety analysis upon which operation of the reactor was licensed. **Figure 3** (on the left) provides a qualitative representation. The dashed,

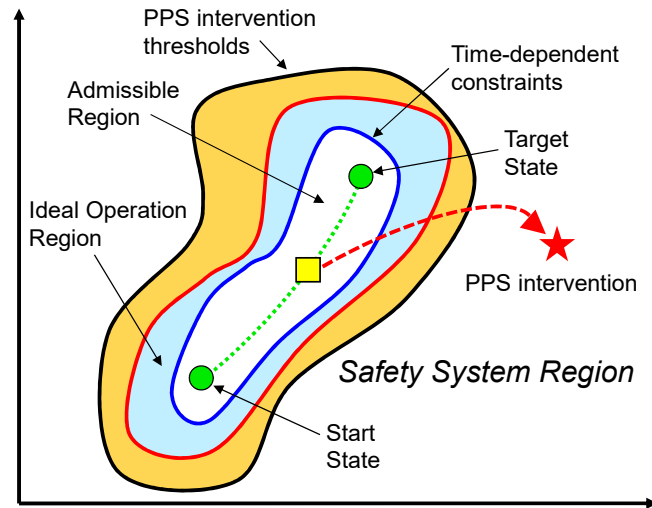
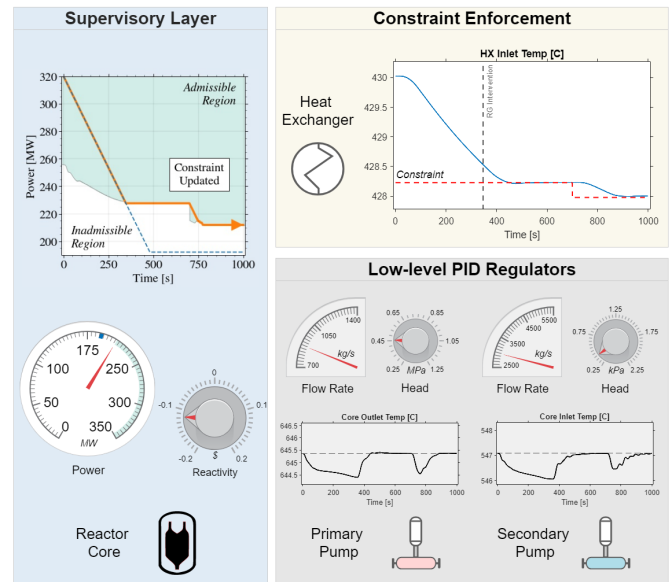


Figure 3. (Above) Qualitative representation of the normal operating envelope. (Right) Graphical user interface of the developed control architecture.

green trajectory describes the plant response during a transient. If some unexpected event occurs (yellow square), the plant state drifts outside the normal operating envelope, the PPS takes over, and the PCS is overridden. Inside the envelope (orange region) is a blue region that represents the ideal operating conditions for sensors and plant components. As performance degrades (e.g., due to sensor bias, fouling, or a reduction in pump hydraulic efficiency, etc.), this region begins to shrink. Though a nuclear unit can still be operated under such conditions, certain operational transients should be avoided so as not to accelerate wear and tear. To this end, the constraints

on the process variables must be adjusted to be made more conservative. These are represented in **Figure 3** by the solid blue line that limits the admissible region. Before initiating a transient, the operator must evaluate sensor and component conditions to ensure that the planned control actions are permitted. This is quite a complicated task, requiring the tight integration of diagnostics and control capabilities. Monitoring the admissible region is key to the autonomous operation paradigm, and is the major focus of this project. In the proposed architecture, different algorithms fulfill this task. As shown in **Figure 1**, beginning with the DIAGNOSTICS-provided updates on the health condition of plant components, DECISION-MAKING determines whether the demanded performance need to be derated, and CONTROL will enforce new constraints by adjusting the setpoint trajectories issued to the low-level controllers.

The project is currently approaching the halfway point of its 3 year timeline. The completed tasks were focused



on modeling and simulation of the plant load-following operation, and on the adaptation of existing control and diagnostics algorithms. Once the high-fidelity model was built, the control strategy was defined and the feedback regulators tuned. This initial portion of the architecture allows for simulating the unit operation in response to sudden demand variations typical of electric grids characterized by high penetration of renewables. In **Figure 3** (on the right), the graphical user interface of the proposed architecture shows the simulation outcomes for a reactor power drop. The performance of the primary circuit controllers, the constraint enforcement, and the evolution of the admissible region during transients are all represented. The next activities will focus on implementation of the diagnostics algorithm and

Continued on next page

integration with the existing control module. Once the different modules are finalized, the final year of the project will mainly focus on the demonstration analysis, with the goal of providing a practical assessment of the designed architecture—from the simulation and diagnosis of component- and sensor-level faults—to the optimization of asset management decisions and the cost-benefit analysis used to evaluate O&M cost reductions.

References

- [1] S. Carpenter, "A Report Undercuts Nuclear Firm's Claims That Its Plants Need Bailouts. But Is It For Real?" *Forbes*, February 1, 2021.
- [2] R. Wood, "Autonomous operation of small reactors: Economy of automation in lieu of economy of scale," *Nuclear News*, July 1, 2021.
- [3] D. Grabaskas, "Cost-Benefit Analyses through Integrated Online Monitoring and Diagnostics," NEUP Project 19-17045, 2019.
- [4] R. B. Vilim, "Process Constrained Data Analytics for Sensor Assignment and Calibration," NEUP Project 18-15179, 2018.
- [5] A. T. Cisneros, "Pebble Bed Reactors Design Optimization Methods and their Application to the Pebble Bed Fluoride Salt Cooled High Temperature Reactor (PBFHR)," Dissertation, UC Berkeley, 2013.
- [6] R. Hu, "SAM Theory Manual," ANL/NE-17/4, Argonne National Laboratory, 2017.
- [7] L. J. Bond, et al., "Improved Economics of Nuclear Plant Life Management," PNNL-SA-56413, Pacific Northwest National Laboratory, 2007.
- [8] S. M. Cetiner, et al., "Development of a Supervisory Control System Concept for Advanced Small Modular Reactors," ASME 2014 Small Modular Reactors Symposium, Washington, DC, April 15–17, 2014.

Novel Cameras for Experiments Inside Nuclear Reactors

Esko Mikkola

Founder & CEO, Alphacore



Alphacore's Vulture and Falcon cameras can operate in high-temperature, high-pressure, and high-radiation environments

Funded by the Department of Energy's Small Business and Innovation Research (SBIR) program, Alphacore is developing a high-frame-rate video sensor and camera that can operate in high-temperature, high-pressure, and high-radiation environments. The novel video camera will significantly improve the state of the art of cameras used in nuclear energy research.

Alphacore's Radiation-Hardened Cameras

When it comes to a camera's radiation tolerance, the image sensor is generally the most sensitive component. While a non-radiation-hardened complex metal-oxide semiconductor (CMOS) image sensor can have very low inherent radiation tolerance (i.e., 3 kilorad, based on Co-60 radiation tests performed by Alphacore), cameras used for nuclear energy applications face significantly higher radiation doses—ranging from hundreds of megarads (Mrad) to gigarads (Grad).

Therefore, Alphacore's approach centers on a custom-designed, radiation-hardened CMOS image sensor for operating within the harsh environments of nuclear energy research. This approach enables the use of low-cost, easy-to-use CMOS technology for such imaging applications, and is a breakthrough product that can potentially accommodate completely new forms of research in nuclear energy, nuclear and high-energy physics, defense nuclear reactor engineering, and many other fields.

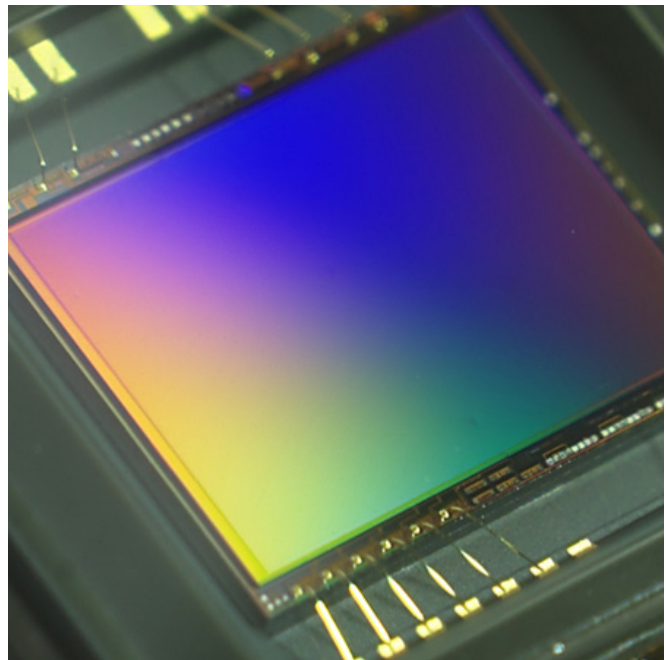
Within this DOE-funded program, Alphacore has focused on two solutions, each based on a different camera architecture:

Vulture: The Vulture camera uses a chip architecture in which every single transistor and sub-circuit are radiation-hardened to the highest possible dose, thus providing over 1 Grad of radiation hardness. The camera can operate at a maximum frame rate range of 60–120 frames per second (fps), with a resolution of 1,024 x 768. It can also operate at higher speeds of 720-1,440 fps, with a decreased resolution of 256 x 256. The maximum frame rate depends on the length of the radiation-hardened cable used to transfer the imaging data from the image sensor to the field programmable gate array (FPGA)-based camera

control and data capture system placed outside the reactor environment. The lower end of the range pertains to a cable length of 40 m.

Falcon: The Falcon camera, a high-speed solution based on Alphacore's advanced ultra-high-frame-rate image sensor architecture, has been optimized using a set of selected radiation-hardening techniques. The Falcon can deliver 5,000 fps with a resolution of 640 x 512, and 20,000 fps with a resolution of 320 x 256.

In almost all high-speed cameras in the world, the image sensor is hosted on a FPGA-based camera control/data-capture board inside the camera enclosure. In Alphacore's cameras, both the sensor and the board will be hardened to the full radiation levels. Alphacore has extensive experience in building commercial off-the-shelf (COTS)-based radiation-tolerant camera boards and then testing



them in radiation chambers. However, according to test results and analyses, a COTS-based approach will not work in light of the radiation levels generated in nuclear energy research, not even close. Moreover, availability of the needed COTS components currently presents a significant challenge.

Thus, Alphacore's approach to an ultra-rad-hard camera is to place all the needed circuitry for power management, data capture, and data transmission on the rigorously hardened CMOS image sensor chip itself. This approach was recently validated by the success of a European slow-

Continued on next page

Continued from previous page

Selected Specifications for the Vulture and Falcon Cameras

Vulture		Falcon	
>100 Mrad Radiation Hardness		>1 Mrad Radiation Hardness	
1,024 x 768	256 x 256	640 x 512	320 x 256
60–120 fps visible wavelength CMOS image sensor	720–1440 fps visible wavelengths CMOS image sensor	5,000 fps visible wavelength CMOS image sensor	20,000 fps visible wavelength CMOS image sensor
Tapeout in August 2022			

frame-rate camera, and Alphacore is the first company/institution in the world that is building an ultra-rad-hard monolithic CMOS chip-based camera for higher frame rates. This “camera-on-a-chip” concept also allows for more straightforward cooling solutions when operating in high-temperature environments.

Applications

Nuclear Research

Alphacore’s technology can be applied toward nuclear-energy-based research projects that study the reactions occurring within a nuclear reactor, and can be used to visualize the conditions a reactor experiences as it operates. At present, experiments are being carried out by simulating nuclear accidents (e.g., fuel assembly breakage) in order to better understand what would happen to the fuel element if it broke, and whether the fuel would bend, bow, or move all over the place^[1].

A key technological need is the ability to observe the reactor during the occurrence of events, as it is challenging to assess events that have already occurred. There is a lack of sensors capable of operating during such events, which occur in the context of extreme environments and thus make it difficult to investigate simulated accidents in terms of fuel rod behavior, neutron exchanges, changes in temperature and pressure, etc.

Another challenge is preserving image resolution when taking video recordings from within the reactor. The solutions currently being explored involve placing a

non-radiation-hardened camera outside the concrete shield of the reactor, then running an imaging fiber up to it. At present, the length of the imaging fiber has been extended to overcome the radiation challenges; however, this causes resolution and image quality degradation, and offers limited radiation tolerance.

In addition, many of the reactions and chemical processes to be observed occur over timescales of microseconds to milliseconds, requiring an imaging solution with a high enough frame rate to capture such fast-occurring phenomena.

The length of the captured video footage is another hurdle. Ideally, the first few tenths of seconds of the experiment can be captured, whereas full tests last anywhere from 100 milliseconds to several minutes. Footage confined to this length prevents the usage of “at sensor” data storage methods, thus necessitating the capability to transfer the high-speed data stream to an external storage location in real time.

The final issue is the cost of the imaging solution. As the camera cannot be removed mid-experiment, the number of times it can be reused varies based on the experiment duration, amount of radiation exposure, and the camera’s robustness against harsh environments. Increasing the useful life of the needed camera will allow for longer, uninterrupted sets of experiments and provide significant cost reduction opportunities.

Alphacore’s radiation-hardened cameras help overcome all these aforementioned challenges, and enable the nuclear energy research community to implement next-generation imaging technology in their experiments. The robust Vulture and Falcon cameras can be placed within harsh reactor environments to capture events—including extremely fast-occurring events—in real time, all while maintaining image resolution/quality and thus helping nuclear scientists gain valuable insights for developing safer and more economic nuclear reactors.



Continued on next page

Continued from previous page

Nuclear Power Plant Inspection and Monitoring

Alphacore's radiation-hardened cameras address certain needs in the nuclear power industry. Many of the camera systems currently being used for nuclear power plant monitoring are cathode ray tube (CRT) cameras, which are generally more radiation-tolerant and require less maintenance than charge-coupled device (CCD) and CMOS image sensor (CIS) technologies.

However, CRT cameras have limitations, including higher maintenance costs and damaged image capture due to burn-in sensitivity, lag, and over-exposure. The high-radiation tolerance and high-resolution imaging capability of Alphacore's Vulture and Falcon cameras can greatly benefit inspection, verification, and repair services for nuclear power plants. The cameras can operate at high temperatures and tolerate extremely high levels of radiation, thus requiring less frequent maintenance or replacement, and reducing costs and downtime. The superior images that can be captured by Alphacore's sensors will also contribute to improvements in quality control services such as fuel monitoring and safety control.

Current Status

Alphacore is currently completing top-level integration of the camera, and the expected tapeout date for the sensors is in August 2022. The sensors will be packaged and ready for testing starting January 2023. The mechanical and firmware designs for the camera will be completed and fabricated by January 2023 as well. The fully integrated system will be evaluated at the beginning of 2023.

About Alphacore

Alphacore's image sensor and camera system designs feature high-resolution and fast frame rates for various stringent performance needs. Designed from the pixel level up, we give our customers flexibility and optimized performance, tailored to fit their needs.

We build image sensors and cameras for harsh radiation and temperature environments. We also provide sensor evaluation kits, that easily characterize and assess image sensor performance prior to integration.

To learn more, visit www.alphacoreinc.com

Acknowledgment

This work was supported by DOE SBIR grant DE-SC0020013.

References

[1] C. Gonzalez, "Slowing Down Nuclear Simulations with High-Speed Cameras," MachineDesign, May 2018, <https://www.machinedesign.com/mechanical/slowng-down-nuclear-simulations-high-speed-cameras>.